Equation of state modules for Waiwera including water, chloride and non-condensible gas

Adrian Croucher[1], Theo Renaud[1], John O'Sullivan[1],Michael O'Sullivan[1] and Jeremy Riffault[1]

[1]Department of Engineering Science, University of Auckland, Private Bag 92019, Auckland 1142, New Zealand

a.croucher@auckland.ac.nz

Keywords: *Reservoir models, numerical modelling, flow simulator, Waiwera, chloride, non-condensible gas*

ABSTRACT

In some geothermal systems there are high concentrations of chloride and some non-condensible gas (mainly CO_2). For reservoir modelling, equation of state (EOS) modules that can handle non-isothermal mixtures of water, chloride and NCGs are required. In the TOUGH2 simulator, EWASG provides a suitable EOS.

In this paper we describe a set of new EOS modules for modelling chloride-rich systems using the parallel, open-source geothermal flow simulator Waiwera. EOS modules for water & chloride, water, chloride & CO_2 and water, chloride & air are provided. Shared code is used to give consistency between results from different EOS modules. The main physical properties of chloride are computed using the updated thermodynamic formulation of Driesner (2007) which also removes the low-temperature limitations of EWASG. As in the pure water and water & NCG EOS modules for Waiwera, primary variable interpolation gives improved phase transition performance and hence faster convergence of natural state simulations.

Some results for theoretical test problems and real high- and low-temperature geothermal fields are presented.

1. INTRODUCTION

Geothermal fluids are generally mixtures of water (liquid or steam), non-condensible gases (NCGs) and dissolved salts. Geothermal reservoir models typically include NCGs such as air, if the unsaturated zone is included in the model, or CO_2 in gas-dominated reservoirs (O'Sullivan et al., 1985).

In many situations dissolved salts are present only in low concentrations and for modelling purposes may be neglected. However, some reservoirs do have appreciable salt concentrations, the predominant form being sodium chloride. In addition, the presence of salt even in relatively low concentrations can have a significant effect on fluid properties and hence flows. It is therefore necessary to be able to include the effects of salt in geothermal reservoir models. For the TOUGH2 and TOUGH3 simulators (Pruess et al., 1999; Jung et al., 2017) and its University of Auckland variant AUTOUGH2 (Yeh et al., 2012), the EWASG EOS module (Battistelli et al., 1997) provides this functionality.

Waiwera is a recently developed parallel, open-source geothermal flow simulator (Croucher et al, 2020), which has now been used to solve a range of geothermal modelling problems (e.g. O'Sullivan et al., 2019; O'Sullivan et al., 2021, Popineau et al., 2022). In the present paper we introduce new equation of state (EOS) modules, including NCGs and sodium chloride, developed for the Waiwera simulator. These new EOS modules were designed to be simpler to use, to be more efficient and to have fewer limitations than comparable EOS modules in other simulators. Here we describe these new Waiwera EOS modules and demonstrate their performance on idealized benchmark problems as well as real geothermal reservoir models.

2. METHODS

2.1 Water & chloride EOS module

An EOS module has two main functions. The first is to take the "primary variables" describing the fluid state in each model grid cell and compute all the required fluid properties (e.g. phase densities, internal energies and viscosities). The second main function of an EOS module is to handle phase transitions.

The EOS module for non-isothermal water and chloride (without NCG) is based on the Waiwera pure water EOS, which can use either the IFC-67 or the IAPWS-97 thermodynamic formulation for water (Wagner et al., 2000). The fluid properties of pure water are modified to account for the presence of chloride. The phase transition handling must also be modified as the chloride affects properties such as saturation pressure.

The assumptions made in formulating the water & chloride EOS are similar to those used in TOUGH2's EWASG EOS (Battistelli et al., 1997). Chloride may be present in dissolved form in the liquid phase, but is assumed to be absent from the vapour phase. When chloride concentrations in the liquid phase exceed a certain solubility limit, chloride may precipitate out into a solid phase (halite). This solid phase is considered immobile and is hence omitted from flux calculations across the faces between model mesh cells. However, the presence of solid halite reduces the effective porosity of the rock. It can also optionally reduce the effective permeability (see Section 2.4). If chloride concentrations decrease again below the solubility limit, the solid halite disappears and is dissolved back into the liquid phase.

The Waiwera water & chloride EOS uses exactly the same primary variables as the pure water EOS (e.g. pressure and temperature in single-phase conditions), but with an additional third variable to represent the chloride. If chloride is present only in the liquid phase, this third variable is the chloride liquid mass fraction. If halite is also present, this is not possible as the chloride liquid mass fraction is given by the solubility of chloride in water. Hence when halite is present the third primary variable is switched to the solid phase saturation (i.e. the volume fraction of halite).

Waiwera uses the concept of "thermodynamic regions" to distinguish different phase conditions simply and unambiguously. These follow the definitions used in the IAPWS-97 thermodynamic formulation for water: region 1 for liquid, region 2 for dry steam and region 4 for two-phase (region 3, supercritical fluid, is not yet included). For the water & chloride EOS this concept is extended by adding another three regions: 5, 6 and 8, respectively, representing liquid, dry steam and two-phase conditions with halite

ISSN 2703-4275

present. Note that these additional regions do not represent different thermodynamic regions as such, as there are no phase transitions in the water component between regions 1 – 4 and the corresponding regions 5 – 8. They are only used to facilitate the necessary change of primary variables when halite is present.

2.2 Chloride thermodynamics

The main thermodynamic properties of brine (water & chloride mixture) are computed using the formulation of Driesner (2007), which gives the density and internal energy (or enthalpy) of brine for a wide range of thermodynamic conditions (pressures from 1 - 5000 bar, temperatures from 0 – 1000 °C and salt mass fractions from 0 – 1). The deviation for low pressures and temperatures (equation 14 in Driesner's paper) and extrapolation for low pressures, high temperatures and high chloride concentrations (equation 17) are implemented. The density and internal energy of solid halite are also computed using the Driesner (2007) formulation.

This removes the limitation of the brine enthalpy formulation of Michaelides (1981) used in TOUGH2's original EWASG, which is inaccurate for temperatures below 100 °C. This limitation has been addressed in later versions of TOUGH2 and TOUGH3 which can also optionally use the Driesner (2007) formulation (Battistelli, 2012).

For the brine saturation pressure equation, the formulation of Haas (1976) is used – the same as is used in EWASG. An updated formulation has been published by Driesner and Heinrich (2007), but this requires a more complex iterative approach, and the Haas (1976) formulation already has adequate accuracy for temperatures below 350 °C (Battistelli, 2012), which is the upper limit for the IFC-67 and IAPWS-97 liquid water thermodynamics formulations.

For brine viscosity, some recent formulations (Mao and Duan, 2009; Klyukin et al., 2017) were considered, but found to give inaccurate results under some conditions. Hence the formulation of Phillips et al. (1981) employed in EWASG is also used in Waiwera.

The formulation for halite solubility is taken from Battistelli (2012), which is available in more recent versions of EWASG and uses a polynomial fit to the formulation given by Driesner and Heinrich (2007), neglecting the small pressure dependence of solubility at temperatures below 400 °C.

2.3 Water, chloride & NCG EOS modules

The EOS modules for non-isothermal water, chloride & NCG (air or CO_2) are based on the water & chloride EOS module and the water & NCG modules. For the most part, the thermodynamics of chloride and NCGs can be treated independently, and so the code for them can be shared by the various EOS modules.

This gives a high degree of consistency between the various Waiwera EOS modules. For example, the water, chloride & NCG modules give exactly the same results as the pure water EOS module when no salt or NCGs are present. This is in contrast with the corresponding TOUGH2 EOS modules which have independent underlying code and often do not give consistent results.

The dissolution of NCG into the liquid phase is affected by the presence of chloride. As in EWASG, this "salting-out" effect is incorporated by multiplying the Henry's law constant by an exponential factor dependent on the chloride mass fraction and the temperature (Battistelli et al., 1997).

The primary variables for the water, chloride & NCG EOS modules are the same as the water & chloride module, with the addition of a fourth variable for NCG. This variable (NCG partial pressure) is the same as the corresponding variable in the water & NCG EOS modules. This makes conversions between the different EOS modules very simple – the addition of chloride and/or NCG to a model only involves adding extra variables, with no changes needed to the existing ones. Again, this is in contrast with the primary variables used by the corresponding TOUGH2 EOS modules, which have little consistency.

2.4 Porosity and permeability modification

As in EWASG, when chloride precipitates out of solution into solid halite the effective porosity is reduced by subtracting the volume fraction of halite, and the effective permeability may also be optionally reduced.

The permeability may be modified according to a simple power-law relation, multiplying the permeability by the porosity reduction factor raised to a specified power. Alternatively, the more complex Verma-Pruess relation can be used (Verma and Pruess, 1988), which considers the possible geometries of the pores and how reduced porosity at the pore throats can have a larger effect on permeability.

As in EWASG, these modifications to porosity and permeability apply both to single-porosity and MINC cells.

2.5 Phase transitions

Waiwera uses an improved primary variable interpolation technique for handling phase transitions (Croucher et al., 2020). When the fluid in a particular numerical cell boils or condenses, a non-linear solution process is used to give an accurate estimate of the point at which the saturation curve is crossed, so that the primary variables (e.g. pressure and temperature) can be interpolated at the crossing point.

For the EOS modules including chloride and/or NCGs, this procedure is extended to include the chloride and the NCG primary variables, which are similarly interpolated at the crossing point. This ensures that these EOS modules retain the improved phase transition behaviour of the pure water EOS. (The addition of chloride also alters the phase transition boundaries, as saturation pressure for brine is used instead of that for pure water.)

3. BENCHMARK TESTS

3.1 Brine - CO_2 column test

This is a 1-D vertical column test based on the CO_2 column problem of O'Sullivan et al. (1985) and also described in Croucher et al. (2017). The 1-D column is 1 km deep with a caprock zone extending to 300 m depth. Here atmospheric conditions of 1 bar and 20 °C are prescribed at the top, and fluid with enthalpy 1800 kJ/kg is injected at the bottom, at 2 kg/s per km^2, with 5% CO_2 mass fraction and 10% chloride mass fraction. The model is started from isothermal hydrostatic initial conditions with no CO_2 or chloride and run to a natural state (time 10^{15} s).

ISSN 2703-4275

Figures 1 – 3 show the natural state Waiwera results vs. elevation for vapour saturation, CO_2 mass fraction and chloride mass fraction. Results from AUTOUGH2 are shown for comparison. The chloride mass fractions reach a maximum of nearly 20% just below the caprock. (This is not high enough for solid halite to begin precipitating out of solution, and so halite results are not shown as they are identically zero.)

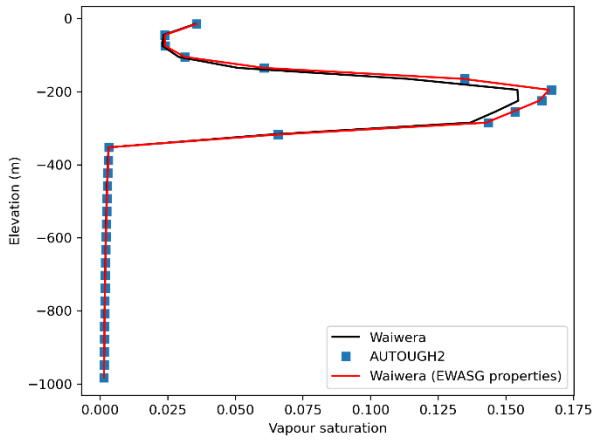


Figure 1: Natural state vapour saturations for brine – CO_2 column test

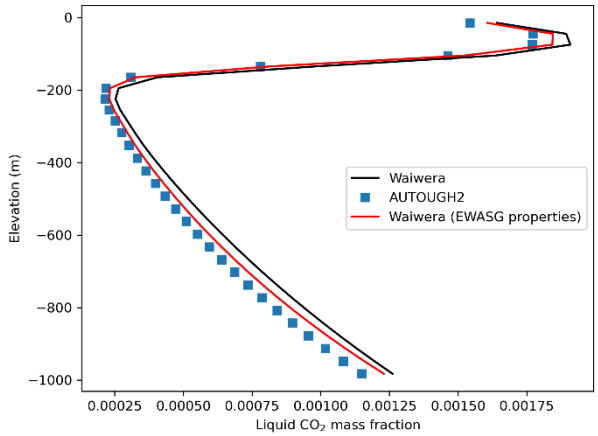


Figure 2: Natural state CO_2 mass fractions for brine – CO_2 column test

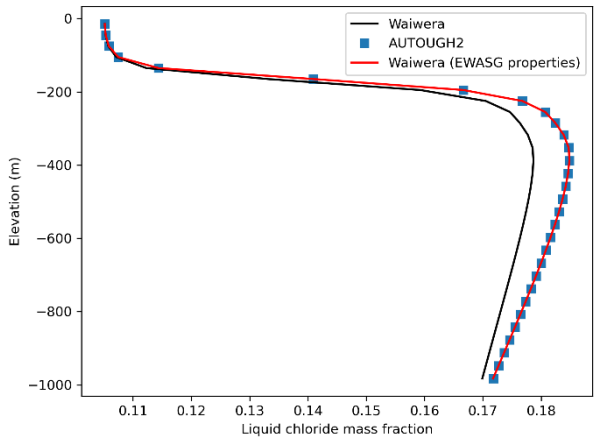


Figure 3: Natural state liquid chloride mass fractions for brine – CO_2 column test

In all three of these plots, the Waiwera and AUTOUGH2 results are similar but there are some significant differences. These are caused by the different chloride thermodynamics formulations used by the two simulators. In fact, the AUTOUGH2 results, which uses the original EWASG formulation, are not strictly valid near the top of the model, where the temperatures drop below 100 °C. Figures 1 – 3 also show a second set of Waiwera results, labelled "Waiwera (EWASG properties)", for which the thermodynamic formulation for brine density and enthalpy was changed from Driesner (2007) to the same formulation used in the original EWASG of AUTOUGH2. This change eliminates almost all of the differences between the AUTOUGH2 and Waiwera results, indicating that they are mainly caused by the modified brine density / enthalpy formulation.

AUTOUGH2 (version 2.46) reached a converged natural state solution in 58 time steps, with six time step size reductions. Waiwera reached natural state in 54 time steps, with no time step size reductions. This is mainly a result of Waiwera's improved phase transition performance (see Section 2.5). For complex large-scale reservoir models this can lead to significant time savings.

3.2 Brine production test with halite precipitation

This problem (loosely based on the "rhbc" sample problem from the TOUGH2 user guide (Pruess et al., 1999)) tests Waiwera's water & chloride EOS by modelling production from a well in a hypersaline geothermal reservoir, with chloride precipitating out into solid halite.

The model mesh is radial with vertical thickness 500 m and 40 cells extending to approximately a 6 km radius. The porosity and permeability are 5% and 50 mD respectively and linear relative permeability curves are used.

The model starts with liquid initial conditions P = 43.2 bar, T = 275.55 °C and chloride mass fraction 35%, just below boiling, and the well is produced at 65 kg/s for 11.5 days. During production the pressures drop, a steam zone forms around the well, chloride increases in concentration and precipitates out into solid halite.

Figures 3 – 5 show the modelled vapour saturation, solid saturation and liquid chloride mass fraction vs radius after 11.5 days. AUTOUGH2 results are shown for comparison. Halite is present within about 20 m of the well; very near the well, it occupies around 50% of the available pore space.

ISSN 2703-4275

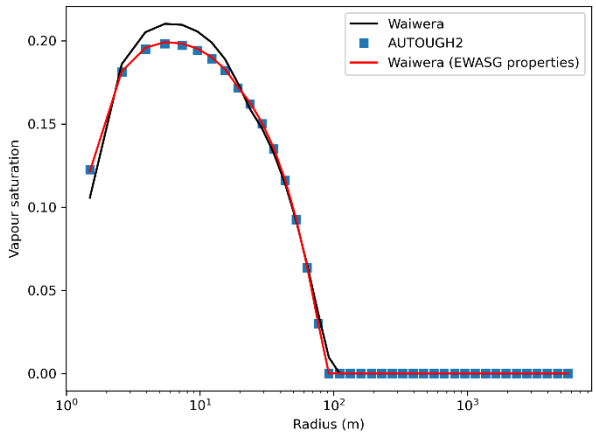


Figure 4: Vapour saturations after 11.5 days for brine production test

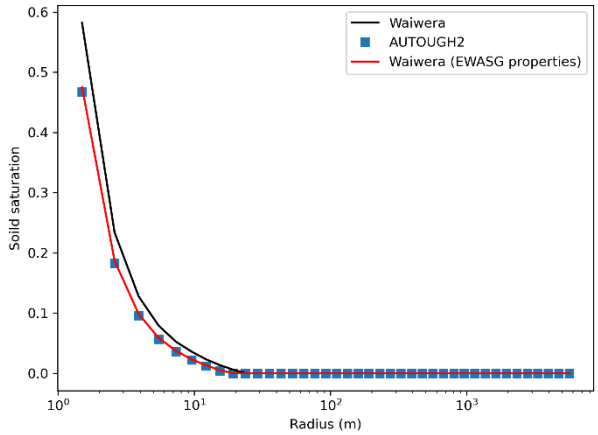


Figure 5: Solid saturations after 11.5 days for brine production test

Once again there are noticeable differences between the Waiwera and AUTOUGH2 results, with Waiwera showing less chloride dissolved in the liquid phase and more precipitating out as halite. Results are also shown for Waiwera with the formulations for brine and halite properties (and halite solubility) switched to those used in AUTOUGH2's EWASG. With these changes the Waiwera and AUTOUGH2 results agree closely, indicating that the differences once again stem from the different thermodynamics used.

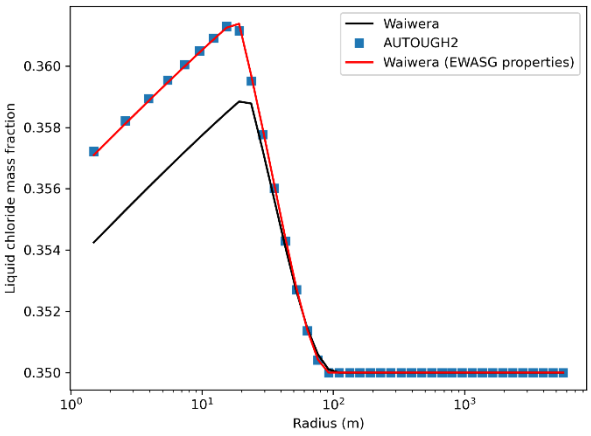


Figure 6: Liquid chloride mass fractions after 11.5 days for brine production test

4. APPLICATIONS

The ability to simulate brine thermodynamics helps to capture complex two-phase processes with dilution, increasing chloride concentration or halite precipitation, involving changes in the mixture enthalpy of the geothermal brines.

Whether for power generation, heat production or mineral extraction (there is a growing interest in lithium extraction), simulating more accurately the properties of the geothermal fluid, instead of just using those of pure water, is likely to become standard practice in the future.

4.1 Synthetic geothermal model

At the University of Auckland, we have developed a synthetic model that we use for teaching. Figure 7 shows the geological model and corresponding reservoir grid (more details in Renaud et al., 2021). This synthetic 3D case is used here to test the water, chloride & CO_2 EOS (WSCE). The models are set with a two-phase surface atmospheric condition with a liquid mass fraction of salt of 1 % and a gas saturation (CO_2) of 98 % for demonstration purposes. Upflows in the bottom layer are set up to generate a hot geothermal plume (Renaud et al., 2021).

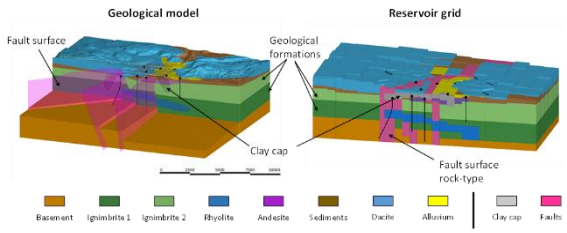


Figure 7: Geological model and Reservoir grid used in the synthetic model (modified from Renaud et al. 2022.)

Figure 8 presents the natural state results in a vertical column of the model for both AUTOUGH2 and Waiwera, with the differences between the two shown in the right column. Note that the Waiwera results have been generated using the IAPWS-97 thermodynamic formulation for water, whereas AUTOUGH2 uses the IFC-67 formulation. Overall, there are absolute temperature differences of less than 0.2°C and only small differences in the salt and CO_2 liquid mass fractions.

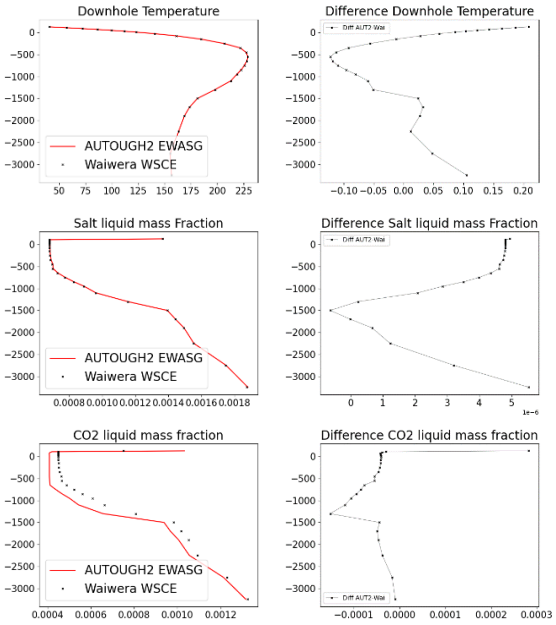


Figure 8: Comparison of AUTOUGH2-EWASG and Waiwera natural state results

4.2 Implications for direct use in sedimentary basins

Popineau et al. (2022) presented a deep sedimentary model of the south Paris area (see Figure 9). It includes 13 geothermal doublets, i.e. one injection and one production well, for district heating. More than 40 years of data were used to calibrate a production history model.

The temperature in the water at the top of the deep aquifer are measured at between 55 and 80°C with a salt concentration of between 6-35 g/l in the exploited brine (Lopez et al., 2010). Figure 10 shows the comparison of the modelled temperature for one well for a simulation using pure water and one including a salt mass fraction of 15%, taken as a mean value from the literature (Lopez et al., 2010). Using the calibrated version presented by Popineau et al. (2022), we observe the effect of salinity is to increase the simulated temperature, giving different results than using pure water as previously presented. This example shows the importance of considering salt concentration in brine, using the water / chloride EOS.

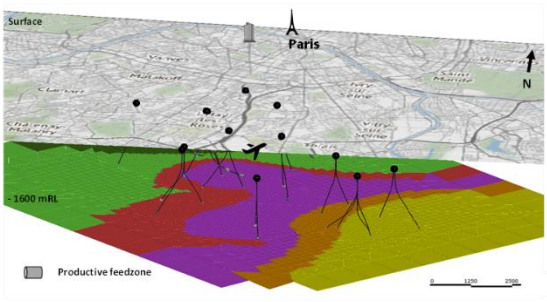


Figure 9: Location of the study area in the south of the Paris urban area in France, intersecting the Paris sedimentary basin (modified Popineau et al. 2022).

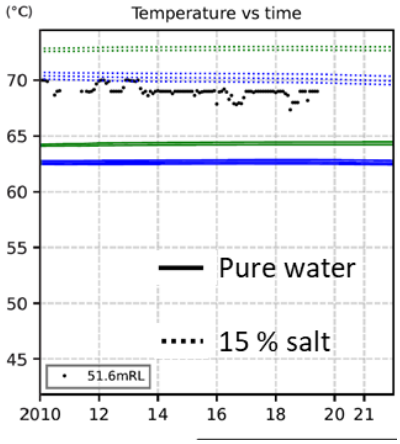


Figure 10: Production temperature comparison in two feedzones (blue and green curves) between 2010 and 2022 for one production well in the Paris Basin area (The black dots are the wellhead temperature field data).

4.3 Hypersaline brines in geothermal systems

Figure 11 shows the location of the Salton Sea area, located in the south of California in the USA. Several active geothermal systems are observed. Shallow cooling intrusions in the areas allowed the development of intense geothermal prospects at depth, with high salt content in the brine (Norton and Hulen, 2006). Deep aquifer supply and a high degree of water-rock interactions resulted in hypersaline brines at depth (Williams and McKibben, 1989).

Araya (2022) built a natural state model of the Salton Sea area. Figures 12 and 13 show the results of the natural state calibration using Waiwera and the water, chloride & air EOS. High concentrations of salt at depth are obtained through mixing processes and deep upflows with variable percentages of salt.

For a model based on publicly available data, Figure 14 presents an example of the calibrated results of a geothermal well in the Salton Sea geothermal area. The data collected for the well chemistry showed an increasing trend in the salt concentration in the brine over time. After calibration, the

ISSN 2703-4275

modelling results agree with the field data with average brine enthalpy of 1000-1500 kJ/kg.

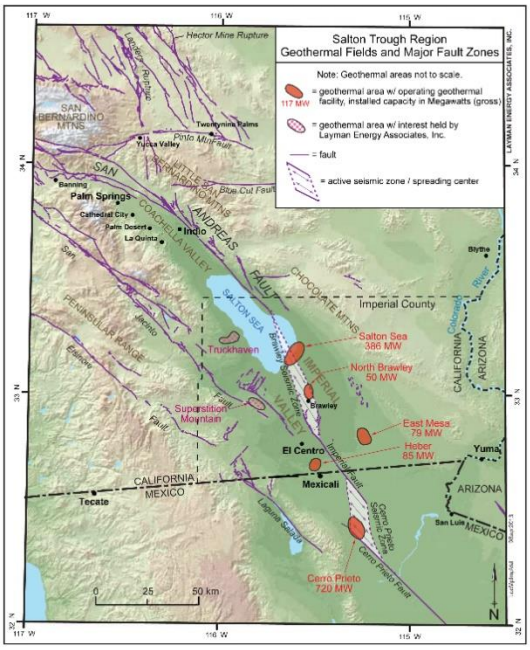


Figure 11: Regional maps of the Salton Sea area with active geothermal systems (from Layman Energy Associates, http://laymanenergy.com).

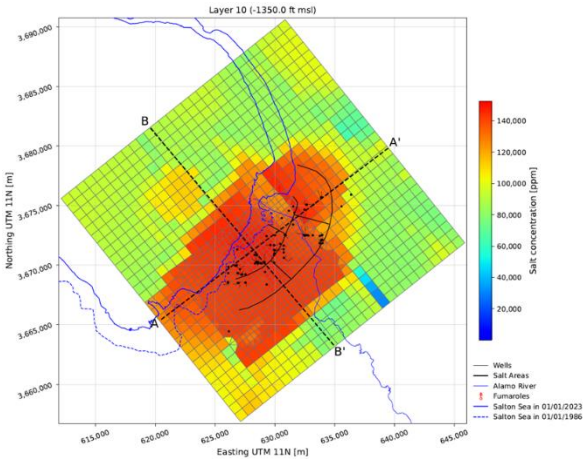


Figure 12: Horizontal layer at the depth of -1350 ft msl showing the calibrated natural state model results for the salt concentration of the Salton Sea model.

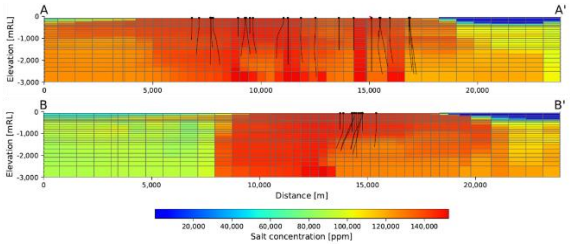


Figure 13: SW-NE and NE-SW cross sections showing the calibrated natural state model results for the salt concentration of the Salton Sea model.

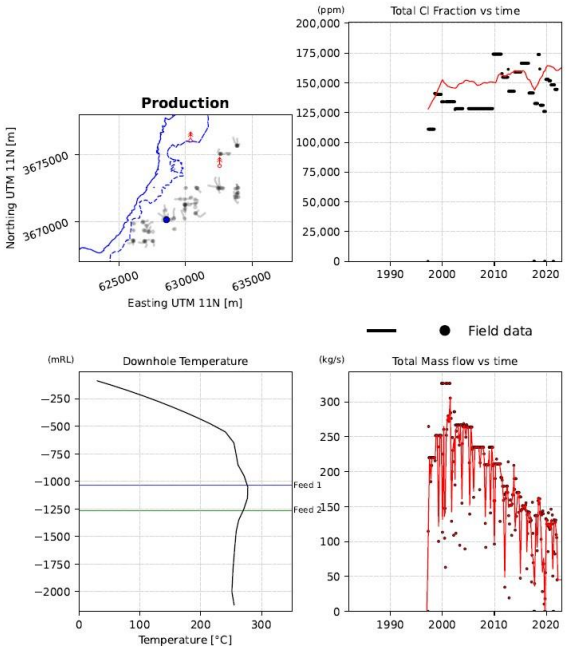


Figure 14: Example of a production history results in one of the Salton Sea production geothermal well.

5. CONCLUSION

Three new equation of state modules have been added to the Waiwera geothermal simulator, for modelling non-isothermal mixtures of water and chloride, with or without NCGs. They feature up-to-date thermodynamic formulations for brine and halite, robust phase transition behaviour and validity over a wide thermodynamic range including low temperatures. Simple and consistent choices of primary variables help to make conversions between different EOS modules straightforward.

Results from benchmark testing and a synthetic teaching model show that Waiwera results computed using these new EOS modules agree well with AUTOUGH2 results, although the updated thermodynamic formulations for brine and halite can make noticeable differences in the results. Modelling applications in real geothermal reservoirs demonstrate the importance of including chloride in both low- and high-salinity settings.

ACKNOWLEDGEMENTS

Waiwera chloride EOS development has been supported by the "Empowering Geothermal" project, funded by the New Zealand Ministry of Business, Innovation and Employment (MBIE). Contact Energy Ltd and Newcrest Mining Ltd have also provided funding throughout the project.

REFERENCES

Araya, N.: *A 3D conceptual and natural-state model of the Salton Sea geothermal field.* Master of Energy Programme, Department of Engineering Science, University of Auckland (2022).

Battistelli, A., Calore, C. and Pruess, K.: The simulator TOUGH2/EWASG for modelling geothermal reservoirs with brines and non-condensible gas. *Geothermics* 26(4), pp. 437 – 464 (1997).

Battistelli, A.: Improving the treatment of saline brines in EWASG for the simulation of hydrothermal systems. *Proceedings, TOUGH Symposium 2012*, Lawrence Berkeley National Laboratory, California (2012).

Croucher, A., O'Sullivan, M., O'Sullivan, J., Pogacnik, J., Yeh, A., Burnell, J. and Kissling, W.: Geothermal Supermodels project: an update on flow simulator development. *Proceedings, 39th New Zealand Geothermal Workshop*, Rotorua, New Zealand (2017).

Croucher, A., O'Sullivan, M., O'Sullivan, J., Yeh, A., Burnell, J. and Kissling, W.: Waiwera: A parallel open-source geothermal flow simulator. *Comp. Geosci*. 141 (2020).

Driesner, T. and Heinrich, C.: The system H2O – NaCl. Part I: Correlation formulae for phase relations in temperature – pressure – composition space from 0 to 1000 °C, 1 to 5000 bar, and 0 to 1 XNaCl. *Geoch. Cosm. Acta* 71, 4880 – 4901 (2007).

Driesner, T.: The system H2O - NaCl. Part II: Correlations for molar volume, enthalpy, and isobaric heat capacity from 0 to 1000 °C, 1 to 5000 bar, and 0 to 1 XNaCl. *Geoch. Cosm. Acta* 71, 4902 – 4919 (2007).

Haas, J.L.: Physical properties of the coexisting phases and thermochemical properties of the H2O component in boiling NaCl solutions. *USGS Bulletin* 1421-A (1976).

Jung, Y., Pau, G., Finsterle, S. and Pollyea, R.: TOUGH3: a new efficient version of the TOUGH suite of multiphase flow and transport simulators. *Comp. Geosci*. 108, 2 - 7 (2017).

Klyukin, Y., Lowell, R. and Bodnar, R.: A revised empirical model to calculate the dynamic viscosity of H2O – NaCl fluids at elevated temperatures and pressures (≤ 1000 °C, 0 - 100 wt % NaCl). *Fluid Phase Equilibria* 433, 193 – 205 (2017).

Lopez, S., Hamm, V., Le Brun, M., Schaper, L, Boissier, F., Cotiche, C., Giuglaris, E.: 40 years of Dogger aquifer management in Ile-de-France, Paris Basin, France. *Geothermics* 39, 339-356 (2010).

Mao, S. and Duan, Z.: The viscosity of aqueous alkali-chloride solutions up to 623 K, 1000 bar, and high ionic strength. *Int. J. Thermophys.* 30, 1510 – 1523 (2009).

Michaelides, E.E.: Thermodynamic properties of geothermal fluids. *Geothermal Resources Council Transactions* 5, 361 – 364 (1981).

Norton, D.L, Hulen J.B.: Magma-hydrothermal activity in the Salton Sea geothermal field, Imperial County, California. *GRC Transactions*, Vol. 30 (2006).

O'Sullivan, M.J. Bodvarsson, G.S., Pruess, K. and Blakeley, M.R.: Fluid and heat flow in gas-rich geothermal reservoirs. Soc. Pet. Eng. J., April 1985, 215 - 226 (1985).

O'Sullivan, J., Croucher, A., Popineau, J., Yeh, A. and O'Sullivan, M.: Working with multi-million block geothermal reservoir models. *Proceedings, 44th Workshop on Geothermal Reservoir Engineering*, Stanford University, Stanford, California (2019).

O'Sullivan, J., Renaud, T., Croucher, A., Yeh, A., Gravatt, M., Riffault, J., Popineau, J. and O'Sullivan, M.: Comparisons of AUTOUGH2 and Waiwera on geothermal fields. *Proceedings, 43rd New Zealand Geothermal Workshop*, Wellington, New Zealand (2021).

Phillips, S., Igbene, A., Fair, J., Ozbek, H. and Tavana, M.: A technical databook for geothermal energy utilization. *Lawrence Berkeley Laboratory Report LBL-12810*, Berkeley, California, 46 pp. (1981).

Popineau, J., Renaud, T., O'Sullivan, J. and Dorado, J.G.: Production history modelling of a low enthalpy geothermal reservoir used for district heating: example of the Paris sedimentary basin. *Proceedings, 44th New Zealand Geothermal Workshop*, Auckland, New Zealand (2022).

Pruess, K., Oldenburg, C. and Moridis, G.: TOUGH2 user's guide, version 2.0. LBNL-43134, Lawrence Berkeley National Laboratory, Berkeley, California (1999).

Renaud, T., Popineau, J., Riffault, J., O'Sullivan, J., Gravatt, M., Yeh, A., Croucher, A., O'Sullivan, M.: Practical workflow for training in geothermal reservoir modelling *Proceedings, 43rd New Zealand Geothermal Workshop*, Wellington, New Zealand (2021).

Verma, A. and Pruess, K.: Thermohydrologic conditions and silica redistribution near high-level nuclear wastes emplaced in saturated geological formations. *J. Geophysical Research* 93, B2, 1159 – 1173 (1988).

Wagner, W., Cooper, J.R., Dittman, A., Kijima, J., Kretzschmar, H.-J., Kruse, A., Mares, R., Oguchi, K., Sato, H., Stöcker, I., Sifner, O., Takaishi, Y., Tanishita, I., Trübenbach, J., Willkommen, Th. : The IAPWS Industrial Formulation 1997 for the thermodynamic properties of water and steam. *ASME J. Eng. Gas Turbines Power* 122, 150–182 (2000).

Williams, A.E., and McKibben, M.A.: A brine interface in the Salton Sea geothermal system, California: fluid, geochemical and isotopic characteristics. *Geoch. Cosm. Acta* 53, 1905-1920 (1989).

Yeh, A., Croucher, A. and O'Sullivan, M.J.: Recent developments in the AUTOUGH2 simulator. *Proc. TOUGH Symposium 2012*, Berkeley, California, September 17-19 (2012).

ISSN 2703-4275